

Report No. 127

October 1972

THE WAVE GENERATED BY A FINE SHIP BOW

T. Francis Ogilvie

This research was carried out under the Naval Ship Systems Command General Hydromechanics Research Program Subproject SR 009 01 01, administered by the Naval Ship Research and Development Center. Contract No. N00014-67-A-0181-0033.

Reproduction in whole or in part permitted for any purpose of the United States Government.

Approved for public release; distribution unlimited.

A stylized graphic of a wave with a white banner across it. The wave is depicted with a thick black outline and a grey stippled interior. The banner is white with black text and is positioned diagonally across the middle of the wave.

THE DEPARTMENT OF NAVAL ARCHITECTURE AND MARINE ENGINEERING

**THE UNIVERSITY OF MICHIGAN
COLLEGE OF ENGINEERING**

THE WAVE GENERATED BY A FINE SHIP BOW

T. Francis Ogilvie

This research was carried out under the
Naval Ship Systems Command
General Hydromechanics Research Program
Subproject SR 009 01 01, administered by the
Naval Ship Research and Development Center.
Contract No. N00014-67-A-0181-0033

Reproduction in whole or in part permitted
for any purpose of the United States Government

Approved for public release; distribution unlimited

Presented at Ninth Symposium on Naval Hydrodynamics
August 1972, Paris



Department of Naval Architecture
and Marine Engineering
College of Engineering
The University of Michigan
Ann Arbor, Michigan 48104

ABSTRACT

The flow field near the bow of a ship has some characteristics of a high-Froude-number problem, even if ship speed is moderate. Some of these features can be predicted by slender-body theory if the usual assumptions of that theory are modified in the bow region to allow for the occurrence of longitudinal rates of change greater than normally assumed. Analytical results are derived for the case of a fine wedge-shaped bow, in which case a universal curve can be drawn for the shape of the bow wave on the hull, regardless of speed, draft, or entrance angle (all within limits, of course). The lengths must be nondimensionalized by the quantity $(HU^2/g)^{1/2}$, where H is the draft, U is ship speed, and g is the gravitation constant. It is shown how this mathematical model matches with the usual slender-body model and how it eliminates certain of the objectionable features of the latter, with only minor complications. Some experimental results are shown which generally confirm the predictions.

CONTENTS

Notation	iv
Figures	v
Introduction	1
The Bow-Flow Problem	6
Solution for a Special Case: A Wedge-Shaped Bow	13
Limit Behavior of the Solution for the Wedge Bow	16
The Usual Slender-Body Solution	22
Comparison of Results with Experiments	26
Critique of the Analysis	36
References	40

NOTATION

$b(x,z)$	hull offset (half-width)
$b(x)$	special case of $b(x,z)$ (the wedge problem)
g	gravitation constant
$H(x)$	draft of the section at x
H	special case of $H(x)$ (the wedge problem)
ℓ	transform variable
L	ship length
r	$(y^2+z^2)^{1/2}$
U	forward speed
x,y,z	coordinates
X	$x\sqrt{\kappa/H}$
α	$b'(0)$, half-angle of the wedge
ϵ	slenderness parameter
$\zeta(x,y)$	free-surface elevation
$Z(X)$	nondimensional $\zeta(x,0)$; see Equation (17).
κ	g/U
ϕ	perturbation velocity potential
$\psi(x,y)$	$\phi(x,y,0)$

FIGURES

Figure 1. Problem for the First Approximation	9
Figure 2. Predicted Bow-Wave Shape on Symmetrical Wedge	27
Figure 3. Bow Wave on a Wedge; Draft = 12 in., Half-Angle = 7.5°	29
Figure 4. Bow Wave on a Wedge; Draft = 12 in., Half-Angle = 15°	30
Figure 5. Bow-Wave Amplitude on Wedge	32
Figure 6. Longitudinal Position of Wave Peak	33
Figure 7. Bow-Wave Amplitude (in Nondimensional Form)	35

INTRODUCTION

The Froude number can be taken as a rough measure of the relative magnitude of inertial forces with respect to gravitational forces in the interior of a fluid region. In the usual problems of ship hydrodynamics, neither of these forces dominates the other in the overall picture, and this fact is recognized in the custom of treating Froude number as a quantity which is $O(1)$ as $\epsilon \rightarrow 0$, where ϵ is the small parameter that provides the reference for ordering all quantities in the problem. If we take as the Froude number $F = U/\sqrt{gL}$, where U is the forward speed, L is ship length, and g is the gravitational acceleration, then the statement that $F = O(1)$ means that there is a characteristic length U^2/g which is comparable with ship length and which is unrelated to the small parameter, ϵ .

In a strict sense, this should always be the case. Suppose that ϵ is a measure of ship thinness or of ship slenderness. As $\epsilon \rightarrow 0$, there is no reason to expect that U^2/g should become either very large or very small; one should certainly be able to specify the forward speed independently of ship thinness or slenderness, and g does not vary significantly in any case.

But there are a couple of reasons sometimes not to accept this apparently natural assumption: a) When we develop an asymptotic analysis, we expect it to be more and more nearly valid as the small parameter becomes infinitesimally small. But we usually obtain just one or two terms in our expansions, and we try to use those expansions for computations when the small parameter is quite finite. We may actually obtain more accurate formulas if we assume an unnatural relationship between ϵ and the length U^2/g . For example, if the latter is actually comparable to ship beam in the cases of practical interest, we may be better off in assuming that $U^2/g = O(\epsilon)$ when we formulate the boundary value problem. b) The implication about the ratio of inertial and gravitational forces may be locally invalid. That is, in some regions, one of these forces may dominate the other to the extent that the asymptotic solution gives grossly wrong predictions in those regions.

The first of these two points I have discussed at length in a previous paper [1]*. In fact, the idea was not original there; it was used many years

*Numbers in square brackets denote references listed at the end of the paper.

earlier by Vossers [2] and also by Joosen [3], for example.

The second point is already implicit in slender-ship theory, for one assumes there that rates of change in the transverse directions are very great compared with rates of change in the longitudinal direction, at least in a region near the ship. This means that accelerations (and thus forces) are greater in one direction than another, and the ratio between them depends on ϵ . Thus, to the extent that we accept slender-ship theory, we have already recognized that the overall Froude number does not characterize the ratio of inertial and gravitational forces uniquely throughout the fluid region.

This idea was also discussed in the earlier work [1] already mentioned. There I pointed out that special order-of-magnitude consideration should be given to conditions near the ship bow. Because of the presence of the free surface, the fluid particles just a very short distance ahead of the bow are quite unaffected by the oncoming ship, until — suddenly! — those particles are in the region of highly accelerated flow around the ship bow. The effects of water displacement by the moving ship are much greater than the effects of gravity, which normally hold the water surface horizontal, and so the presence of the free surface is momentarily simply equivalent to a pressure-relief surface. All of this can be implied by saying that the flow near the ship bow is a high-Froude-number flow.

Thus we come to the concept that the bow flow is a high-Froude-number problem, even if the ship speed is moderate. The previous argument then suggests that we try to relate the Froude-number aspect of the bow flow to the slenderness parameter. In this paper, I have done this in a very pragmatic way:

In the usual slender-body theory, we assume, in a symbolic notation, that $\partial/\partial x = O(1)$ but that $\partial/\partial y$ and $\partial/\partial z = O(1/\epsilon)$, where x is the longitudinal coordinate. This means that rates of change in the longitudinal direction are smaller than rates of change in the transverse direction by an order of magnitude ϵ . (It is this very gradual variation in the longitudinal direction that leads to the typical feature of the slender-ship near field, namely, that the free surface acts as a rigid wall. Rates of change are so gradual that gravity

dominates and holds the free surface horizontal.) This intuitive picture is formalized in the mathematics by stretching coordinates in the transverse directions by a factor $1/\epsilon$.

Now we suppose that, near the bow, rates of change of the flow variables should be greater than those usually assumed in slender-body theory. We may expect to introduce such a notion formally by stretching the x coordinate from the bow sternward. But what should be the degree of stretching? Let us define a new longitudinal coordinate, $X = x/\epsilon^n$, with x and X both measured from the bow in the downstream direction. If $n = 0$, we have the usual slender-body theory, and if $n = 1$ we have the original problem in three dimensions. (In the latter case the stretching is isotropic.) Therefore we seek a value of n such that $0 < n < 1$. It turns out that a nontrivial problem arises only if $n = 1/2$, and so I make such an assumption in this paper.

The resulting theory is still a slender-body theory, in that the first approximation involves a Laplace equation in the two transverse dimensions only. The rates of change in the near field are much greater in the transverse direction than in the longitudinal direction, but the difference in order of magnitude between them is less than in the usual slender-body theory.

One can describe the theory as being valid (presumably) in a region just behind the bow in which $x = O(\epsilon^{1/2})$, where x is measured in units such that ship length is $O(1)$. It will be convenient sometimes to speak of a "bow near field," by which I shall mean an asymptotically defined region in which $x = O(\epsilon^{1/2})$ and $r = (y^2+z^2)^{1/2} = O(\epsilon)$. In the "usual near field," we assume that $x = O(1)$ and $r = O(\epsilon)$, whereas in the far field all variables are $O(1)$ (which means simply that we can fix our attention on a point in the fluid and the point is not supposed to move as $\epsilon \rightarrow 0$).

Some interesting things happen in the bow near field. We no longer have the rigid-wall free-surface condition which is typical of the usual near field. Instead, we find exactly the same linear free-surface conditions that are familiar from classical thin-ship theory, for example. But the partial differential equation is the Laplace equation *in two dimensions*, as in ordinary slender-body theory. This means that we must solve an equation in the variables y and z , with boundary conditions involving derivatives with respect to x .

The explicit solution of this problem is presented for the case of a thin, wedge-shaped bow. The shape of the wave along the side of the body has been computed, and experiments were conducted for comparison with the predictions. The results are in fair agreement.

From the analysis, it can be concluded that an appropriate length for purposes of nondimensionalization is the geometric mean of two lengths, the draft and the characteristic length, $\lambda/2\pi = U^2/g$. That is, we refer all lengths to $(HU^2/g)^{1/2}$, where H is the draft of the forebody. The extent to which the experimental data then collapse into simple curves is quite remarkable. Even in cases of very low forward speed, in which the analysis fails completely, the same data collapse still appears to occur.

The conditions to be satisfied in the bow near field automatically match with the conditions in the usual near field of slender-body theory. So it is not surprising that the solutions also match automatically, in the sense of the method of matched asymptotic expansions. We can say that the new analysis actually encompasses the usual slender-ship theory, in that the formulas and equations of the new analysis include all of the terms in the corresponding expressions, plus some extra terms that would be considered as of higher order, in the usual theory.

It is quite striking how the solution of the bow-near-field problem goes over into the solution for the usual slender-body near field: In a region extremely close to the bow, the flow has the character expected of a high-Froude-number flow, i.e., the fluid velocity is mostly perpendicular to the plane of the undisturbed free surface. However, as $x/\epsilon^{1/2} \equiv X \rightarrow \infty$, the fluid velocity at the plane of the undisturbed free surface becomes approximately parallel to that plane. The wave elevation alongside the body changes order of magnitude in this transition: Wave elevation is $O(\epsilon^{3/2})$ in the bow near field, but it is $O(\epsilon^2)$ in the usual slender-ship near field; the present analysis shows how this change takes place.

Finally, it should be mentioned that this analysis probably contains no information that is not inherent in a thin-ship analysis. However, the information which is available from the present analysis is quite easily obtainable,

in contrast to the usual situation with thin-ship calculations. For example, the calculation of wave profile along the side of the ship was carried out in a few hours with a desk calculator! Also, there are other possible applications of the ideas contained herein, applications which would probably not be feasible with thin-ship theory as a starting point. For example, Hirata [4] has treated the case of a cambered thin ship (actually with zero thickness) and Baba [5] has analyzed a flat ship by this basic method. The latter problem was partly anticipated by Maruo [6].

THE BOW-FLOW PROBLEM

Let the ship be travelling in the negative x direction, the origin of coordinates being fixed to the bow. The z axis points upwards. The ship geometry is defined by the formula:

$$y = \pm b(x,z) ,$$

where the non-negative function $b(x,z)$ is the hull offset corresponding to the point $(x,0,z)$ on the ship centerplane. The free surface shape is given by the formula:

$$z = \zeta(x,y) ,$$

defined for $|y| > b(x,0)$.

It is assumed that the ship is "slender," which means that there is a small parameter, ϵ , characterizing the smallness of beam/length and draft/length ratios. As $\epsilon \rightarrow 0$, the ship shrinks down to a line, the part of the x axis between the origin and $x = L$, L being the ship length at the waterline. But "slenderness" means more than this. It implies also that the size and shape of hull cross-sections change gradually in the longitudinal direction. In particular, we shall require that:

$$\frac{\partial b}{\partial x} = O(\epsilon) , \quad 0 < x < L ,$$

even in the bow near field.

The "bow near field" is defined as the region in which:

$$x = O(\epsilon^{1/2}) , \quad r = (y^2+z^2)^{1/2} = O(\epsilon) .$$

It is assumed that, in the bow near field, the flow variables are changed in order of magnitude when they are differentiated, according to the following symbolic rules:

$$\frac{\partial}{\partial x} = O(\epsilon^{-1/2}) ; \quad \frac{\partial}{\partial r} , \quad \frac{\partial}{\partial y} , \quad \frac{\partial}{\partial z} = O(\epsilon^{-1}) .$$

These effects could be brought about formally through the introduction of new

variables, $x = X\epsilon^{1/2}$, $y = Y\epsilon$, $z = Z\epsilon$, after which we would require that differentiation with respect to X , Y , and Z have no effect on orders of magnitude. However, the rules will simply be carried along implicitly, the introduction of such new variables being quite unnecessary.

Note that there is one exception to the above procedure: We have already required that $b(x,z) = O(\epsilon)$ and $\partial b(x,z)/\partial x = O(\epsilon)$. This is simply a condition on hull geometry. It has nothing to do with the nature (or existence) of a flow around the ship.

We assume everything that is necessary for the existence of a velocity potential, which we write in the following form:

$$Ux + \phi(x,y,z) .$$

As usual, the potential satisfies the Laplace equation in the fluid domain:

$$[L] \quad 0 = \phi_{xx} + \phi_{yy} + \phi_{zz} .$$

$$[\phi/\epsilon] \quad [\phi/\epsilon^2] \quad [\phi/\epsilon^2]$$

The expressions in square brackets give the orders of magnitude in the bow near field of the terms immediately above. Although we do not yet know the order of magnitude of ϕ , it is already clear that we can ignore the term ϕ_{xx} in finding the first approximation to the solution in the bow near field.

The boundary condition on the hull can be written:

$$0 = \pm Ub_x \pm \phi_x b_x - \phi_y \pm \phi_z b_z \quad \text{on} \quad y = \pm b(x,z) .$$

$$[\epsilon] \quad [\phi\epsilon^{1/2}] \quad [\phi/\epsilon] \quad [\phi/\epsilon]$$

Dropping the one term which is clearly of negligible order of magnitude, we can rewrite this condition:

$$[H] \quad \frac{\partial \phi}{\partial n} \sim \frac{\pm \phi_y - b_z \phi_z}{\sqrt{1 + b_z^2}} \sim \frac{U b_x}{\sqrt{1 + b_z^2}} = O(\epsilon) .$$

Since the operator $\partial/\partial n$ is similar to, say, $\partial/\partial r$ with respect to its effect on orders of magnitudes, we can now conclude that either $\phi = O(\epsilon^2)$ or the first approximation to ϕ satisfies a homogeneous boundary condition on the

In finding the first approximation to ϕ , we have a boundary-value problem to solve in the y - z plane. That is, we have a partial differential equation involving only the transverse rates of change. The body boundary condition is a simple Neumann condition, but the free-surface condition involves derivatives with respect to x , and so a 3-D aspect is introduced through this condition. The problem in the cross plane is illustrated in Figure 1(a).

For the moment, we shall confine our attention to a special case of this problem, namely, to narrow bodies which can be generated approximately by a distribution of sources on the centerplane, $y = 0$. This special case is depicted in Figure 1(b). A modification of our method of solution has been worked out for more general cases, but we shall not consider such cases further in the present paper; they would only distract us from the simple ideas which are being developed.

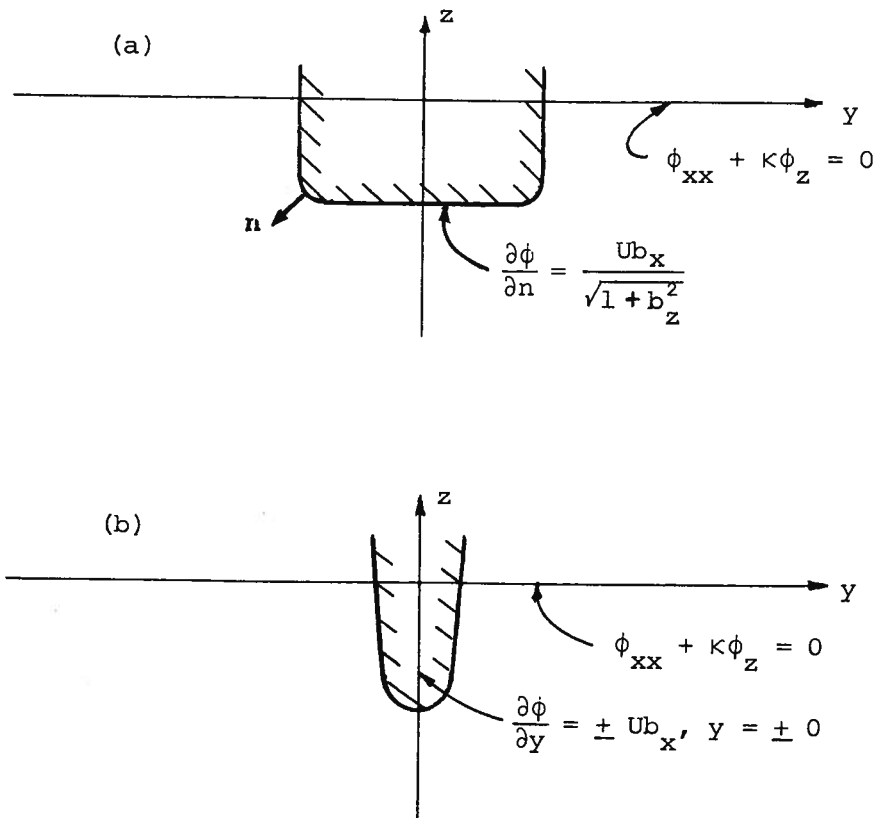


Figure 1. Problem for the First Approximation.

(a) General Body. (b) Thin Body.

In both cases, the potential satisfies: $\phi_{yy} + \phi_{zz} = 0$.

For the thin bodies being considered, we shall suppose that the body boundary condition can be expressed:

$$\frac{\partial \phi}{\partial n} \approx \pm \frac{\partial \phi}{\partial y} \approx Ub_x \quad \text{on } y = \pm 0, \text{ for } z > -H(x).$$

The following 2-D potential function satisfies this body boundary condition:

$$\text{Re} \left\{ -\frac{U}{\pi} \int_{-H(x)}^0 d\zeta b_x(x, \zeta) \log(y + iz - i\zeta) \right\}.$$

In fact, if we let v and w respectively denote the corresponding velocity components in the y and z directions, we find easily that:

$$v - iw = \frac{U}{\pi} \int_{-H(x)}^0 \frac{d\zeta}{i\zeta - (y + iz)} b_x(x, \zeta).$$

For $y = \pm 0$, this can be evaluated through use of the Plemelj formula:

$$(v - iw)|_{y=\pm 0} = \pm Ub_x(x, z) + \frac{U}{i\pi} \int_{-H(x)}^0 \frac{d\zeta b_x(x, \zeta)}{\zeta - z}.$$

Thus,

$$v(x, \pm 0, z) = \pm Ub_x(x, z),$$

as required.

The above potential function satisfies the partial differential equation and the body boundary condition. To that potential, we can add the potential for any other source distribution which induces no net normal velocity component on $y = 0$, $-H(x) < z < 0$. We choose to write $\phi(x, y, z)$ in the following fashion:

$$\begin{aligned} \phi(x, y, z) = \text{Re} \left\{ +\frac{U}{\pi} \int_{-H(x)}^0 d\zeta b_x(x, \zeta) \log(y + iz - i\zeta) \right. \\ \left. - \frac{U}{\pi} \int_0^{H(x)} d\zeta b_x(x, -\zeta) \log(y + iz - i\zeta) \right. \\ \left. - \frac{1}{\pi i} \int_{-\infty}^{\infty} \frac{d\eta \psi(x, \eta)}{\eta - (y + iz)} \right\}. \end{aligned} \quad (1)$$

The quantity in braces is a function of the complex variable $(y+iz)$. The y and z components of velocity are obtained easily:

$$\phi_y - i\phi_z = -\frac{U}{\pi} \int_{-H(x)}^0 \frac{d\zeta b_x(x,\zeta)}{i\zeta - (y+iz)} + \frac{U}{\pi} \int_0^{H(x)} \frac{d\zeta b_x(x,-\zeta)}{i\zeta - (y+iz)} - \frac{1}{\pi i} \int_{-\infty}^{\infty} \frac{d\eta \psi_\eta(x,\eta)}{\eta - (y+iz)}$$

If we require only that

$$\psi(x,y) = \psi(x,-y) ,$$

the boundary condition on $y = \pm 0$ is satisfied, for the last term above is purely imaginary on $y = 0$, and the next-to-last term represents a source distribution on the centerplane above $z = 0$. Furthermore, if we approach the plane of the undisturbed free surface from below, we find that:

$$\lim_{z \uparrow 0} \phi(x,y,z) = \psi(x,z) , \quad (2)$$

which will be an important fact in the analysis ahead.

The first two integrals in (1) represent the flow due to a line of [2-D] sources on the negative z axis and a line of sinks symmetrically located on the positive z axis. Together they cause only a vertical flow at the plane of the undisturbed free surface, $z = 0$. The third integral in (1) can represent a flow with both vertical and horizontal components at the plane $z = 0$.

We now substitute the above potential function into the free-surface condition, [F]:

$$\begin{aligned} 0 &= \phi_{xx} + \kappa \phi_z \\ &= \psi_{xx} - \frac{2U\kappa}{\pi} \int_{-H(x)}^0 \frac{d\zeta \zeta b_x(x,\zeta)}{\zeta^2 + y^2} - \frac{\kappa}{\pi} \int_{-\infty}^{\infty} \frac{d\eta \psi_\eta(x,\eta)}{\eta - y} \end{aligned}$$

Rewritten slightly, this is an integro-differential equation for $\psi(x,y)$:

$$\psi_{xx} - \frac{\kappa}{\pi} \int_{-\infty}^{\infty} \frac{d\eta \psi_{\eta}(x, \eta)}{\eta - y} = \frac{2U\kappa}{\pi} \int_{-H(x)}^0 \frac{d\zeta \zeta b_x(x, \zeta)}{\zeta^2 + y^2} . \quad (3)$$

The next task is to solve this equation for $\psi(x, y)$. When that has been done, we can use (1) to express $\phi(x, y, z)$.

The above equation applies to thin bodies of rather general shape; there is not much restriction on the function $b(x, z)$. Rather than try immediately to solve this general problem, I have decided that it was more important to determine first the degree of validity of the fundamental assumptions that were made. For this reason, I shall next concentrate on one special case, for which the solution is easily obtained. We can then compare the predictions of this analysis with the results of experiments and determine whether it is worthwhile to solve Equation (3) for more general shapes.

SOLUTION FOR A SPECIAL CASE: A WEDGE-SHAPED BOW

We now restrict our attention to wedgelike bodies. In the bow near field, in which $x = O(\epsilon^{1/2})$, we assume that the body shape is given by:

$$y = \pm b(x) , \quad -H < z < 0 .$$

As before, we assume that $b = O(\epsilon)$ and also that $b'(x) = db/dx = O(\epsilon)$. A consequence is that in the bow near field we have:

$$b(x) = b(0) + x b'(0) + \frac{1}{2} x^2 b''(0) + \dots .$$

$$[\epsilon^{3/2}] \quad [\epsilon^2]$$

For a wedgelike entrance, $b(0) = 0$, and so we have, approximately,

$$y = \pm x\alpha [1 + o(1)] , \quad -H < z < 0 , \quad (4)$$

as the description of the body, where $\alpha = b'(0)$, the wedge half-angle. This argument might have been used previously to justify the thin-body approximation, although one might question whether it would be more convincing than the simple statement of assumption made previously. However, now it serves a much more practical purpose: We can simplify the right-hand side of Equation (3). In the bow near field, the integro-differential equation becomes:

$$\psi_{xx} - \frac{\kappa}{\pi} \int_{-\infty}^{\infty} \frac{d\eta \psi_{\eta}(x, \eta)}{\eta - y} = -\frac{\kappa U \alpha}{\pi} \log \frac{H^2 + y^2}{y^2} . \quad (5)$$

At first sight, this equation appears rather formidable. But the integral can be considered as a convolution integral, a fact which suggests the use of Fourier transforms to eliminate the y dependence. In what follows, we manipulate some transforms which are nonsense in a classical analysis; whenever necessary, integrals should be interpreted in the sense of generalized functions. We follow Lighthill [7] in such respects.

Let the Fourier transform be defined as follows:

$$F\{f(y)\} = f^*(\ell) = \int_{-\infty}^{\infty} dy e^{-i\ell y} f(y) ;$$

$$F^{-1}\{f^*(\ell)\} = f(y) = \frac{1}{2\pi} \int_{-\infty}^{\infty} d\ell e^{i\ell y} f^*(\ell) .$$

The transform of the right-hand side of Equation (5) can be computed as follows:

$$\begin{aligned} \int_{-\infty}^{\infty} dy e^{-i\ell y} \log \frac{H^2 + y^2}{y^2} &= \int_{-\infty}^{\infty} dy e^{-i\ell y} [\log (y-iH) + \log (y+iH) - 2 \log |y|] \\ &= \frac{1}{i\ell} \int_{-\infty}^{\infty} dy e^{-i\ell y} \left(\frac{1}{y-iH} + \frac{1}{y+iH} \right) + 2\pi i \frac{\text{sgn } \ell}{i\ell} \\ &= \frac{2\pi}{|\ell|} [1 - e^{-H|\ell|}] . \end{aligned}$$

The integral term in Equation (5) can be treated as an ordinary convolution integral, with the result that:

$$\begin{aligned} \int_{-\infty}^{\infty} dy e^{-i\ell y} \left(-\frac{\kappa}{\pi} \int_{-\infty}^{\infty} \frac{d\eta \psi_{\eta}(x, \eta)}{\eta - y} \right) \\ = -\frac{\kappa}{\pi} [i\ell \psi^*(x; \ell)] [\pi i \text{sgn } \ell] = \kappa |\ell| \psi^*(x; \ell) . \end{aligned}$$

The integro-differential equation now becomes an ordinary differential equation with respect to x :

$$\psi_{xx}^*(x; \ell) + \kappa |\ell| \psi^*(x; \ell) = -\frac{2\kappa U \alpha}{|\ell|} \left\{ 1 - e^{-H|\ell|} \right\} . \quad (6)$$

The solution of this equation is now readily obtained. A particular solution is the following:

$$\begin{aligned} \psi^*(x; \ell) &= -\frac{2U\alpha}{\ell^2} \left\{ 1 - e^{-H|\ell|} \right\} \left\{ 1 - \cos \sqrt{\kappa|\ell|} x \right\} \\ &= \phi^*(x; \ell; 0) \quad (\text{by Equation (2)}) . \end{aligned} \quad (7)$$

In principle, we should include the complementary solution, and this would be easy enough to do. However, the above solution appears to suffice for all that follows.

There seems to be little point in writing out the corresponding expression for $\phi(x,y,z)$, which could be done through use of Equation (1). In fact, we shall not even bother at this point to write out the inverse transform of the expression in (7), although we note that the latter can be expressed in terms of Fresnel integrals. It is worthwhile to write at least the transforms of two related quantities, namely, $\phi_z^*(x;l;0)$ and $\phi_x^*(x;l;0)$:

$$\phi_z^*(x;l;0) = \frac{2U\alpha}{|l|} \left(1 - e^{-H|l|}\right) \cos \sqrt{\kappa|l|} x \quad ; \quad (8)$$

$$\phi_x^*(x;l;0) = -\frac{2U\alpha}{l^2} \sqrt{\kappa|l|} \left(1 - e^{-H|l|}\right) \sin \sqrt{\kappa|l|} x \quad . \quad (9)$$

The behavior of ϕ_z^* at large distance from the bow will be interesting to note presently, and ϕ_x^* is essentially the transform of the wave height, which can be seen from the dynamic free-surface condition [A].

LIMIT BEHAVIOR OF THE SOLUTION FOR THE WEDGE BOW

Behavior as $|y| \rightarrow \infty$. Since the potential and its derivatives on the plane $z = 0$ are all given in terms of Fourier transforms with respect to y , it is nearly a trivial matter to determine how the inverse transforms act when $y \rightarrow \pm \infty$. We need only to examine the behavior of the transforms near their singularities. The only singularities occur at $\ell = 0$. For example, $\phi_z^*(x; \ell; 0)$ can be expressed:

$$\begin{aligned} \phi_z^*(x; \ell; 0) &= 2U\alpha \left\{ H - \frac{1}{2} H^2 |\ell| + \dots \right\} \left\{ 1 - \frac{1}{2} \kappa |\ell| x^2 + \dots \right\} \\ &= 2U\alpha H \left[1 - |\ell| \left\{ \frac{H}{2} + \frac{1}{2} \kappa x^2 \right\} + \dots \right]. \end{aligned}$$

Treating this transform as a generalized function, we can obtain the limit behavior of its inverse transform by using the methods described by Lighthill [7]. We find that:

$$\phi_z(x, y, 0) = \frac{U\alpha H (H + \kappa x^2)}{\pi y^2} + \dots \quad \text{as } y \rightarrow \infty.$$

This shows that, far off to the sides, the disturbance appears to be caused by a vertical dipole distribution. Such a result should not be too surprising, since the body boundary condition was satisfied by distributing sources over the underwater part of the centerplane, to which we added a distribution of opposite sinks on the abovewater image of the centerplane. These two distributions alone would certainly lead to the dipole-like behavior far off to both sides. Apparently, the third term in the expression for ϕ , as given in (1), has negligible influence in this sideways limit.

Actually, we guaranteed such a result by choosing the complementary solution as we did in (7). Effectively, we have implied that there are no waves upstream of the bow, even in the bow near field. In the final section, we shall return to this point; it requires much more study in the future.

The transform of the wave deformation function can be expressed:

$$\zeta^*(x; \ell) = - \frac{U}{g} \phi_x^*(x; \ell; 0),$$

and, from (9), this quantity has the following behavior near $\ell = 0$:

$$\begin{aligned}\zeta^*(x; \ell) &= \frac{2\alpha}{|\ell| \sqrt{\kappa|\ell|}} \left(1 - e^{-H|\ell|}\right) \sin \sqrt{\kappa|\ell|} x \\ &= 2\alpha H x \left\{1 - |\ell| \left[\frac{H}{2} + \frac{\kappa x^2}{6}\right] + \dots\right\}.\end{aligned}\quad (10)$$

The inverse transform then must have the behavior:

$$\zeta(x, y) = \frac{0Hx}{\pi y^2} \left[H + \frac{\kappa x^2}{3}\right] + \dots \quad \text{as } |y| \rightarrow \infty.$$

It can be shown that the potential itself drops off inversely with y^2 , but this does not seem to provide any special insight into the results.

Behavior as $x \rightarrow \infty$. This is an important limit, for it provides the connection to the usual slender-body solution. Let us recall that $x = O(\epsilon^{1/2})$ in the bow near field region. Our solution, when we let $x \rightarrow \infty$, should match the solution of the usual slender-body problem if we let $x \rightarrow 0$ in the latter.

In order to obtain these limits, we manipulate the inverse transforms into forms so that the generalized-function procedures can again be used. For the vertical component of velocity, for example, we go through the following steps:

$$\begin{aligned}\phi_z(x, y, 0) &= \frac{1}{2\pi} \int_{-\infty}^{\infty} d\ell e^{i\ell y} \left\{ \frac{2U\alpha}{|\ell|} \left(1 - e^{-H|\ell|}\right) \cos \sqrt{\kappa|\ell|} x \right\} \\ &= \frac{2U\alpha}{\pi} \int_0^{\infty} d\ell \cos \ell y \left(\frac{1 - e^{-H\ell}}{\ell} \right) \cos \sqrt{\kappa\ell} x \\ &= \frac{4U\alpha}{\pi} \int_0^{\infty} d\lambda \cos \lambda x \cos \frac{y\lambda^2}{\kappa} \left(\frac{1 - e^{-H\lambda^2/\kappa}}{\lambda} \right) \\ &= \frac{2U\alpha}{\pi} \int_{-\infty}^{\infty} d\lambda e^{i\lambda x} \cos \frac{y\lambda^2}{\kappa} \left(\frac{1 - e^{-H\lambda^2/\kappa}}{|\lambda|} \right) \\ &\sim - \frac{4U\alpha H}{\pi \kappa x^2} \quad \text{as } x \rightarrow \infty.\end{aligned}\quad (11)$$

The interpretation of this result is of some interest. The quantities α and H are each of order ϵ . In addition, $x = O(\epsilon^{1/2})$ in the bow near field. Thus, $\phi_z = O(\epsilon)$ in the bow near field. Now, we have already commented that the solution in the bow near field must match the solution given by the usual slender-body theory. In fact, the near field of the usual slender-body theory is a far field with respect to the bow region; $x = O(1)$ in the usual theory. From this point of view, the expressions obtained above for ϕ_z represent a one-term inner expansion, and the final formula above is the one-term outer expansion of the one-term inner expansion. In matching it with the corresponding "far field," we must reinterpret the variables as far-field variables and re-order the expansion. In the present case, this means only that we revise our estimate by considering x to be $O(1)$, in which case we observe that $\phi_z = O(\epsilon^2)$ on the plane $z = 0$ as $x \rightarrow \infty$. This agrees with the well-known result of the usual slender-body theory. We shall say more about this presently.

What is most remarkable about the above result is the manner in which the flow completely changes its character in the downstream direction. Very close to the bow, the flow appears to have been caused by a distribution of vertical dipoles, and so the flow at the plane $z = 0$ is almost completely normal to the plane. However, as $x \rightarrow \infty$, we find that the normal component of velocity on the plane $z = 0$ vanishes and the flow becomes parallel to the plane.

We also examine how the wave elevation varies asymptotically in the downstream direction. We proceed as with ϕ_z : We write ζ as the inverse transform of the expression in (10) and then manipulate it so that it appears formally to be a transform with respect to x . We obtain in this way:

$$\begin{aligned}
 \zeta(x,y) &= \frac{2\alpha}{\pi i} \int_{-\infty}^{\infty} d\lambda e^{i\lambda x} \operatorname{sgn} \lambda \cos \frac{y\lambda^2}{\kappa} \left(\frac{1 - e^{-H\lambda^2/\kappa}}{\lambda^2} \right) \\
 &\sim \frac{2\alpha H}{\pi i \kappa} \int_{-\infty}^{\infty} d\lambda e^{i\lambda x} \operatorname{sgn} \lambda \left[1 - \frac{H\lambda^2}{2\kappa} + \dots \right] \\
 &\sim \frac{4\alpha H}{\pi \kappa x} + O(1/x^5) \quad \text{as } x \rightarrow \infty .
 \end{aligned} \tag{12}$$

It is worth noting that the y dependence enters only in the term which drops off inversely with x^5 . We also observe that $\zeta = O(\epsilon^{3/2})$ in the bow near

field, where we assume that $x = O(\varepsilon^{1/2})$, but when we re-interpret x as being $O(1)$ we must conclude that $\zeta = O(\varepsilon^2)$. This is in agreement with the well-known results of the usual slender-body theory.

Finally, we obtain an estimate for $\phi(x, y, 0)$ as $x \rightarrow \infty$. The transform of this quantity was given in Equation (7). It is clear that we cannot follow exactly the same procedure as we did for estimating ϕ_z or ζ , since there is a part of the expression in (7) which does not even depend on x . However, we can proceed in two steps:

(a) First we consider the part of the transform in (7) that does not depend on x , namely, the quantity:

$$-\frac{2U\alpha}{\ell^2} \left(1 - e^{-H|\ell|} \right).$$

We shall find that this is the transform of

$$\operatorname{Re} \left\{ \frac{U\alpha}{\pi} \int_{-H}^H d\zeta \log (y+iz - i\zeta) \right\} \Big|_{z=0}. \quad (13)$$

The interpretation of this result will be discussed after we prove that it is true. By elementary means, we obtain the following result:

$$\begin{aligned} \operatorname{Re} \left\{ \frac{U\alpha}{\pi} \int_{-H}^H d\zeta \log (y+iz - i\zeta) \right\} \Big|_{z=0} \\ &= \frac{U\alpha}{2\pi} \int_{-H}^H d\zeta \log (y^2 + \zeta^2) \\ &= \frac{U\alpha}{\pi} \left[H \log (H^2 + y^2)/y^2 + H \log y^2 + 2 [y \cot^{-1}(y/H) - H] \right]. \end{aligned}$$

The last expression is now broken into several pieces, for each of which we obtain the generalized Fourier transform. For the first piece, the transform exists even in the classical sense:

$$\begin{aligned} \int_{-\infty}^{\infty} dy e^{-i\ell y} \log \frac{H^2 + y^2}{y^2} &= 2 \int_0^{\infty} dy \cos \ell y \log \frac{H^2 + y^2}{y^2} \\ &= \frac{2\pi}{|\ell|} \left(1 - e^{-H|\ell|} \right). \end{aligned}$$

From the point of view of generalized functions, we have the following result:

$$\int_{-\infty}^{\infty} dy e^{-i\ell y} \log y^2 = -\frac{2\pi}{\ell} \operatorname{sgn} \ell = -\frac{2\pi}{|\ell|} .$$

One more integral can be computed readily:

$$\begin{aligned} \int_{-\infty}^{\infty} dy e^{-i\ell y} [y \cot^{-1}(y/H) - H] &= 2 \int_0^{\infty} dy \cos \ell y [y \cot^{-1}(y/H) - H] \\ &= -\frac{2}{\ell} \int_0^{\infty} dy \sin \ell y \left(\cot^{-1} \frac{y}{H} - \frac{yH}{y^2+H^2} \right) \\ &= -\frac{\pi}{\ell^2} + \frac{\pi}{\ell^2} e^{-H|\ell|} [1 + H|\ell|] . \end{aligned}$$

These three transforms can now be combined to yield the result stated above, that is,

$$-\frac{2U\alpha}{\ell^2} \left(1 - e^{-H|\ell|} \right) = \frac{U\alpha}{\pi} \int_{-\infty}^{\infty} dy e^{-i\ell y} \left[H \log (H^2+y^2) + 2[y \cot^{-1}(y/H) - H] \right] .$$

The expression in (13) is the potential for the flow caused by a line distribution of sources on the centerplane and on the above-water image of the centerplane, the potential having been evaluated on $z = 0$. We recall that we started constructing our solution, in Equation (1), by assuming that there was a distribution of sources on the submerged part of the centerplane and a distribution of opposite sinks on the image of the centerplane. We now discover the interesting fact that one part of the potential, when evaluated on the plane of the undisturbed free surface, represents a symmetrical distribution of singularities, rather than an antisymmetrical distribution. The symmetrical distribution would have been a logical starting point in the ordinary slender-body theory, in which a rigid-wall free-surface condition must be satisfied. It appears in the present analysis as a natural consequence in the region downstream of the bow region, although we started with quite a different picture of the flow around the bow.

(b) The remaining part of the expression in (7) is oscillatory with respect to x , and so we use the procedure that worked well in estimating the downstream behavior of ϕ_z and ζ . We go through the following steps:

$$\begin{aligned}
 & \frac{1}{2\pi} \int_{-\infty}^{\infty} d\ell \, e^{i\ell y} \frac{2U\alpha}{\ell^2} \left(1 - e^{-H|\ell|}\right) \cos \sqrt{\kappa|\ell|} x \\
 &= \frac{2U\alpha}{\pi} \int_0^{\infty} d\ell \, \cos \ell y \left[\frac{(1 - e^{-H|\ell|}) \cos \sqrt{\kappa\ell} x}{\ell^2} \right] \\
 &= \frac{2U\alpha\kappa}{\pi} \int_{-\infty}^{\infty} \frac{d\lambda}{\lambda^3} e^{-i\lambda x} \operatorname{sgn} \lambda \cos \frac{y\lambda^2}{\kappa} \left[1 - e^{-H\lambda^2/\kappa}\right] \\
 &\sim -\frac{4U\alpha H}{\pi} \log Cx + O(1/x^2) \qquad \text{as } x \rightarrow \infty,
 \end{aligned}$$

where C is a constant which cannot be determined from this analysis.

From the two-part analysis above, we obtain our desired result, the estimate of the potential on $z = 0$ as $x \rightarrow \infty$:

$$\phi(x, y, 0) \sim \operatorname{Re} \left\{ \frac{U\alpha}{\pi} \int_{-H}^H d\zeta \log (y - i\zeta) \right\} - \frac{4U\alpha H}{\pi} \log Cx + O(1/x^2)$$

as $x \rightarrow \infty$. (14)

Thus, we see that the potential represents the source distribution already discussed, in addition to which there is a term which becomes infinite logarithmically when x goes to infinity. These results will both appear in a proper perspective when we consider what the usual slender-body theory predicts near the bow. Both of the explicit terms above are $O(\epsilon^2 \log \epsilon)$ in the bow near field.

The appearance of the constant, C , in the above result is an unfortunate consequence of our use of generalized-function theory. In general, the value of the constant may even have to change as the formulas are manipulated. From a strict mathematical point of view, it is quite improper to leave a final formula in such a shape that it can be interpreted only in terms of generalized functions, especially when it is supposed to have direct physical significance. Fortunately, this is not so much of a problem for us here as might be supposed. The quantities with real physical significance are ϕ_z and ζ , and their estimates are not at all murky.

THE USUAL SLENDER-BODY SOLUTION

If one stretches coordinates near the body in such a way that:

$$x = X, \quad y = \epsilon Y, \quad z = \epsilon Z$$

and then treats derivatives with respect to the new variables as if they had no effect on orders of magnitude, one obtains the usual problem and solution of slender-body theory. Without going through the formalism of such changes of variables, we write down directly the boundary-value problem that results for the wedge-like body that we are considering in this paper. The first approximation to the near-field perturbation potential satisfies the following:

$$[L] \quad \phi_{yy} + \phi_{zz} = 0 ;$$

$$[H] \quad \left\{ \begin{array}{l} \frac{\partial \phi}{\partial y} = \pm Ub'(x) \quad \text{on } y = \pm b(x) , \\ \frac{\partial \phi}{\partial z} = 0 \quad \text{on } z = -H ; \end{array} \right.$$

$$[A] \quad \left. \begin{array}{l} g\zeta + U\phi_x + \frac{1}{2} \phi_y^2 = 0 \\ \phi_z = 0 \end{array} \right\} \quad \text{on } z = 0 .$$

The last condition, [B], is of course the rigid-wall condition which replaces the free-surface condition. The dynamic boundary condition on the free surface, [A], serves only for the determination of the free-surface shape, ζ , after the potential problem is solved. In the body boundary condition, we have stated a separate condition for the bottom of the wedge, for we do not need or want to restrict ourselves to a "thin" slender-body over the entire body length.

The above problem can be solved precisely, by mapping, for example. We do not need that complete solution, however. Let $\Phi(x,y,z)$ be the solution of this 2-D problem which has the property:

$$\Phi(x,y,z) \sim \frac{2UHb'(x)}{\pi} \log |y^2+x^2|^{1/2} \quad \text{as } |y^2+z^2|^{1/2} \rightarrow \infty .$$

Then the perturbation potential, $\phi(x,y,z)$, is given by:

$$\phi(x,y,z) = \Phi(x,y,z) + F(x) ,$$

where $F(x)$ is given by [8]:

$$F(x) = \frac{U}{2\pi} \int_{-\infty}^{\infty} d\xi s''(\xi) \left\{ \operatorname{sgn}(x-\xi) \log 2|x-\xi| + \frac{\pi}{2} H_0(\kappa(x-\xi)) \right. \\ \left. + (2 + \operatorname{sgn}(x-\xi)) \frac{\pi}{2} Y_0(\kappa|x-\xi|) \right\} ,$$

where $s(x)$ is the area of the immersed part of the cross-section at x , Y_0 is the Bessel function of the second kind, and H_0 is a Struve function. (Notation is the same as in [9].) Near the bow, we note that:

$$s(x) = \begin{cases} 0 & x < 0 , \\ 2\alpha Hx + \dots & 0 < x , \end{cases}$$

where the "... " denotes some smooth function of x . The first and second derivatives of $s(x)$ can then be expressed as follows:

$$s'(x) = \begin{cases} 0 & x < 0 , \\ 2\alpha H + \dots & 0 < x ; \end{cases}$$

$$s''(x) = 2\alpha H\delta(x) + \dots ,$$

where $\delta(x)$ is the Dirac delta function.

The function $F(x)$ represents the effects of interactions between the various cross-sections. For a body in an infinite fluid, we would have just the first term in the integrand, and one can show easily that it represents the flow on the x axis caused by a distribution of sources both upstream and downstream of the point under consideration. The other two terms represent the effects of the free-surface, and they combine with the logarithm term in such a way as to cancel any flow upstream of a source. Tuck [8] has shown this explicitly. The integrand of the $F(x)$ expression has a wavelike nature for $\xi < x$ but not for $\xi > x$.

We are interested in how the above solution behaves as $x \rightarrow 0$. In fact, the easiest procedure for determining this behavior is to treat x as being

$O(\epsilon^{1/2})$ and re-order all quantities accordingly. When we do this (after much algebra, expanding of the Bessel functions, etc.), we find that:

$$F(x) \sim -\frac{4UH\alpha}{\pi} \left[\log x + \frac{1}{4} \log \frac{\kappa^3}{4} + \frac{3}{4} \gamma \right], \quad \text{for } x = O(\epsilon^{1/2}),$$

where γ is Euler's constant. The problem for $\bar{\phi}$ becomes, for $x = O(\epsilon^{1/2})$, a wedge-flow problem, with a rigid wall in place of the free surface; its solution is:

$$\bar{\phi}(x,y,z) = \text{Re} \left\{ \frac{U\alpha}{\pi} \int_{-H}^H d\zeta \log (y+iz - i\zeta) \right\}. \quad (15)$$

When we combine the two results above, we obtain a one-term expansion of the potential, to be matched with the bow-near-field expansion:

$$\phi(x,y,z) \sim \text{Re} \left\{ \frac{U\alpha}{\pi} \int_{-H}^H d\zeta \log (y+iz - i\zeta) \right\} - \frac{4U\alpha H}{\pi} \log Cx,$$

where

$$\log C = \frac{1}{4} \log \frac{\kappa^3}{4} + \frac{3}{4} \gamma.$$

This result should be compared with that in (14): the matching is perfect, with the previously unknown constant C now fixed. The interpretation is, of course, different. In (14), the potential was approaching infinity logarithmically as $x \rightarrow \infty$; here, the potential is approaching infinity logarithmically as $x \rightarrow 0$.

The kinematic free-surface condition, [B], does not mean that ϕ_z is precisely equal to zero on the plane $z = 0$; it means only that $\phi_z|_{z=0} = 0$ for the leading-order term in the solution for ϕ . The first approximation to ϕ is $O(\epsilon^2)$ and the first approximation to ϕ_z is $O(\epsilon)$. Thus, the statement that $\phi_z|_{z=0} = 0$ really means that $\phi_z|_{z=0} = o(\epsilon)$. This remains true even as $x \rightarrow 0$. Thus, the first-order term in ϕ_z automatically has the correct behavior for matching with (11), which gave the behavior of ϕ_z in the bow near field, under the condition that $x \rightarrow \infty$.

Finally, we consider once more the wave-shape function, $\zeta(x,y)$. From the dynamic boundary condition, [A], combined with what we have found above concerning the slender-body potential for this problem, we can express ζ in the following way:

$$\zeta(x,y) = -\frac{U}{g} \Phi_x - \frac{U}{g} F'(x) - \frac{1}{2g} \Phi_y^2, \quad \text{on } z = 0.$$

For the wedge-shaped bow, with constant draft, we can find immediately that $\Phi_x \approx 0$. (See (15).) For x very small, we also find easily that:

$$F'(x) \approx -\frac{4UH\alpha}{\pi x}$$

The final term needed is the one involving Φ_y , this quantity being:

$$\Phi_y = \operatorname{Re} \left\{ \frac{U\alpha}{\pi} \int_{-H}^H \frac{d\zeta}{i\zeta - (y+iz)} \right\} + \dots,$$

the remainder being a quantity which goes to zero at the bow. We need to evaluate this quantity only on $z = 0$, for which we find:

$$\Phi_y \approx \frac{2U\alpha}{\pi} (\operatorname{sgn} y) \tan^{-1} \frac{H}{|y|}.$$

We now have the following representation for the wave shape:

$$\zeta(x,y) \sim -\frac{4H\alpha}{\pi Kx} - \frac{2\alpha^2}{\pi^2 K} \left[\tan^{-1} \frac{H}{|y|} \right]^2 = O(\epsilon^2).$$

The last estimate of order of magnitude is still valid in the usual near field, where $x = O(1)$. In order to match this result with the bow-near-field formula, we must reinterpret the order of magnitude of x , that is, consider that $x = O(\epsilon^{1/2})$, and re-order the expansion. When we do this and keep just one term, we have only:

$$\zeta(x,y) \sim -\frac{4H\alpha\alpha}{\pi Kx} = O(\epsilon^{3/2}).$$

We now observe that this matches precisely with the expression in (12).

COMPARISON OF RESULTS WITH EXPERIMENTS

From Equation (10), we can compute the shape of the free-surface disturbance:

$$\begin{aligned}\zeta(x,y) &= \frac{\alpha}{\pi} \int_{-\infty}^{\infty} d\ell e^{i\ell y} \left(\frac{1 - e^{-H|\ell|}}{|\ell|} \right) \left(\frac{\sin(\sqrt{\kappa|\ell|x})}{\sqrt{\kappa|\ell|}} \right) \\ &= \frac{2\alpha}{\pi} \int_0^{\infty} d\ell \cos \ell y \left(\frac{1 - e^{-H\ell}}{\ell} \right) \left(\frac{\sin \sqrt{\kappa\ell} x}{\sqrt{\kappa\ell}} \right) .\end{aligned}\quad (16)$$

For $y = 0$, this simplifies further:

$$\zeta(x,0) = \frac{2\alpha}{\pi} \int_0^{\infty} d\ell \left(\frac{1 - e^{-H\ell}}{\ell} \right) \left(\frac{\sin \sqrt{\kappa\ell} x}{\sqrt{\kappa\ell}} \right) \quad (16')$$

We obtain our simplest form when we make the following changes of variables:

$$x = x \sqrt{\kappa/H} , \quad Z(X) = \frac{\pi}{2\alpha} \sqrt{\frac{\kappa}{H}} \zeta(x,0) . \quad (17)$$

Equation (16') now collapses into the following:

$$Z(X) = \int_0^{\infty} d\mu \left(\frac{1 - e^{-\mu}}{\mu} \right) \left(\frac{\sin \sqrt{\mu} X}{\sqrt{\mu}} \right) . \quad (18)$$

Thus, the wave along the side of the wedge can be nondimensionalized in such a way that we have a single universal curve, a function of just one variable, which purports to describe the wave shape for any speed, any draft, and any wedge angle. Of course, we have not yet considered the range of validity of these results, but it is clear that they are very simple results.

It is worthwhile to notice the manner in which the length scales are made nondimensional: The reference length is $(H/\kappa)^{1/2} = (HU^2/g)^{1/2}$. This is the geometric mean of two lengths, the draft H and characteristic free-surface length U^2/g .

Also, the wedge half-angle enters in a very simple way: The non-dimensional wave height, Z , must be multiplied by the ratio, $\alpha/(\pi/2)$ (in addition to being made dimensional on the scale of $(H/\kappa)^{1/2}$). Thus, the theory predicts that wave height along the side of the wedge will be proportional to the wedge angle.

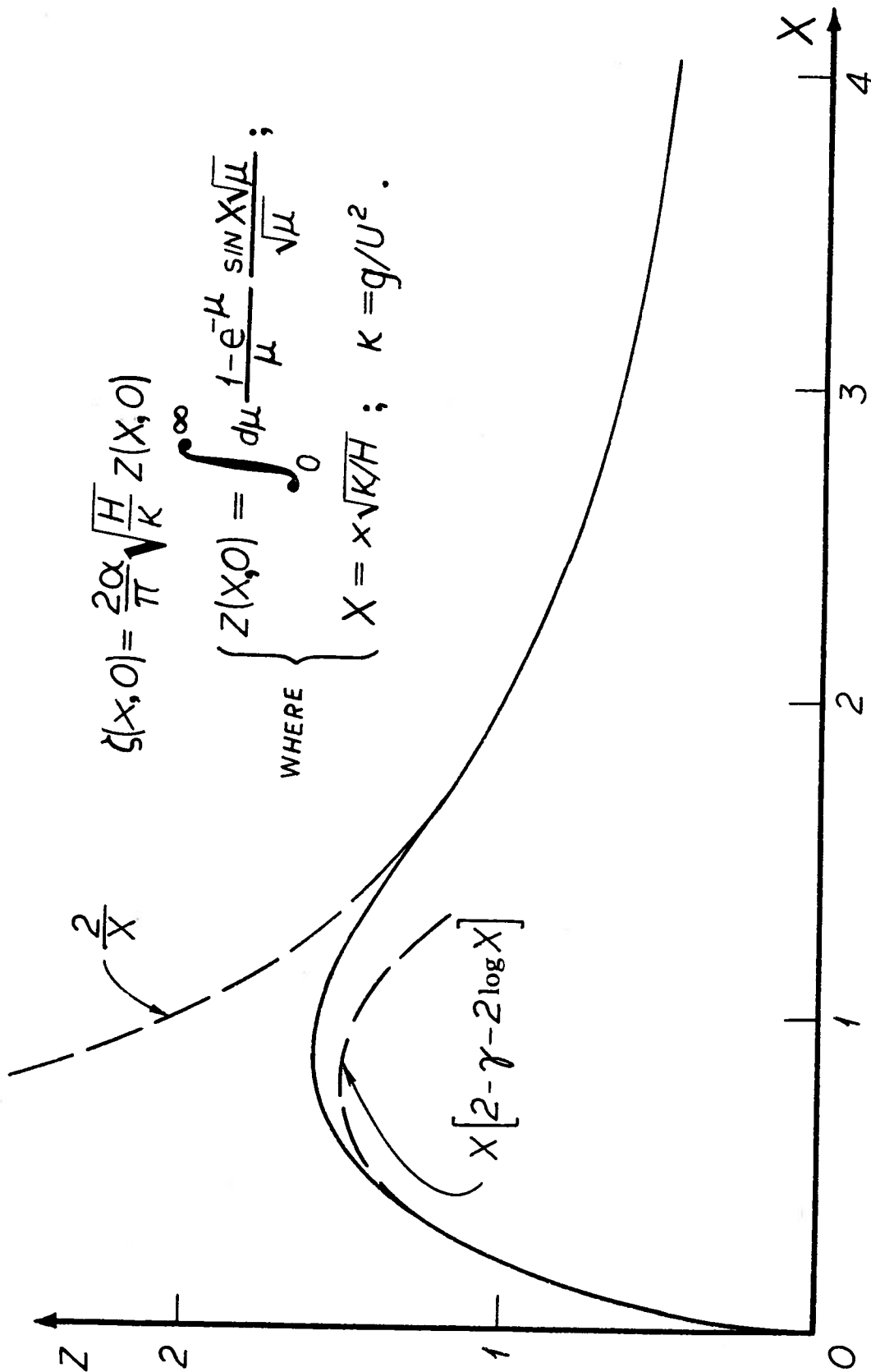


FIGURE 2. PREDICTED BOW-WAVE SHAPE ON SYMMETRICAL WEDGE

Calculation of $Z(X)$ has been carried out, with the results shown in Figure 2. In addition, the integral in (18) has very simple asymptotic approximations which are valid as $X \rightarrow 0$ or $X \rightarrow \infty$, and these are shown by the broken curves in Figure 2.

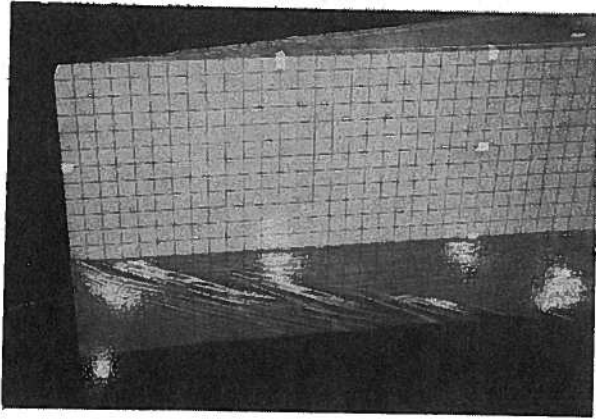
In order to determine whether this result was even approximately valid, we conducted some experiments with a very simple model. The planform of the model was that of an unsymmetrical diamond; at one end, the model was a wedge with a half-angle of 7.5° , and at the other end the half-angle was 15° . Tests were conducted at speeds up to about 15 ft./sec., with drafts from 4 in. to 16 in. A grid had been inscribed on the model so that wave shapes could be measured from photographs of the bow wave.

In Figures 3 and 4, two selected series of tests are shown. In both figures, the model is being tested at a draft of 12 in.

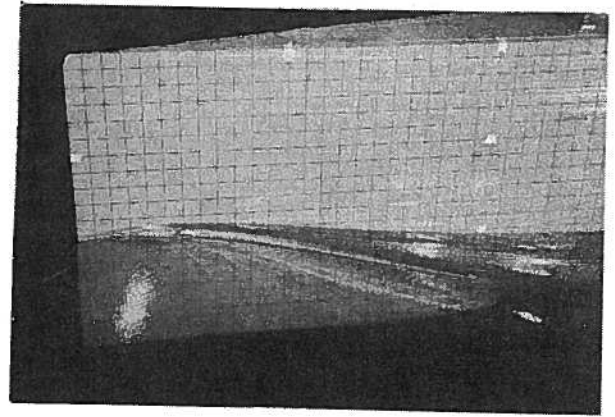
There are several qualitative features in these photographs that are worth noting:

(i) The model speed in Figure 3(a) is 1.64 ft./sec., which is only about twice the minimum speed at which waves can travel on a water/air interface. (Minimum speed is about 23.2 cm./sec.) In fact, capillary waves are quite evident in this picture, as well as in several of the higher-speed test pictures. Whether these ripples can actually be seen apparently depends more on the lighting than on anything else. The existence of a sharp edge on the model presumably accentuated the amplitude of the ripples in all of our tests.

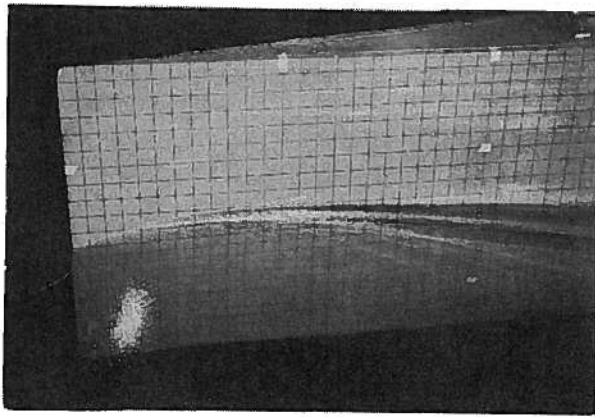
(ii) In (b) - (e) of Figure 3, the water level at the bow edge is about 1 in. above still-water level. (The white mark at the bow is at the 18 in. draft mark, and the squares are 1 in. on a side.) This rise of water level ahead of the bow is, of course, not predicted in the analysis. We fully expected to observe such a rise, and we recognized that it would represent a source of error in the predictions. What we did not anticipate was that the rise is quite insensitive to forward speed. From a speed of about 5 ft./sec. (Figure 3(b)) to a speed in excess of 15 ft./sec. (Figure 3(e)), this rise increases from about 0.8 in. to about 1.2 in.



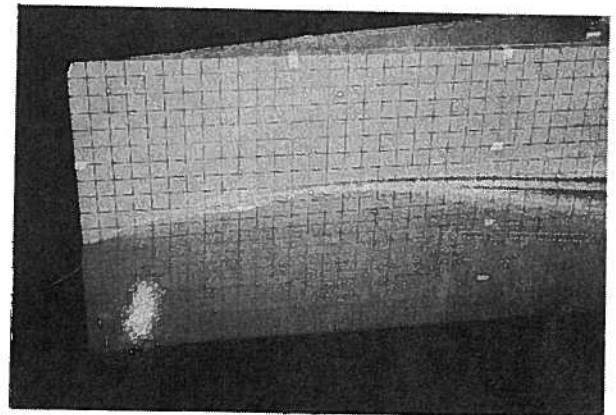
$U = 1.64$ ft./sec.



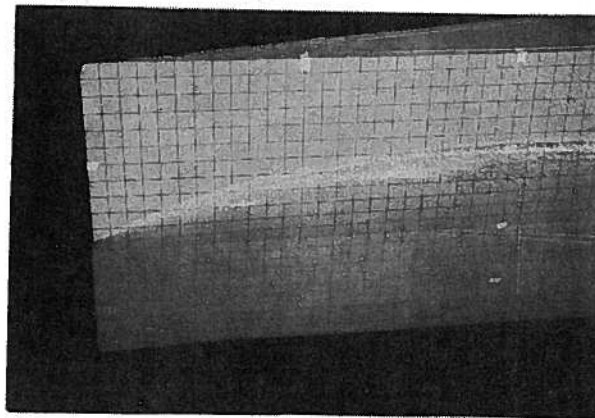
$U = 4.95$ ft./sec.



$U = 8.22$ ft./sec.

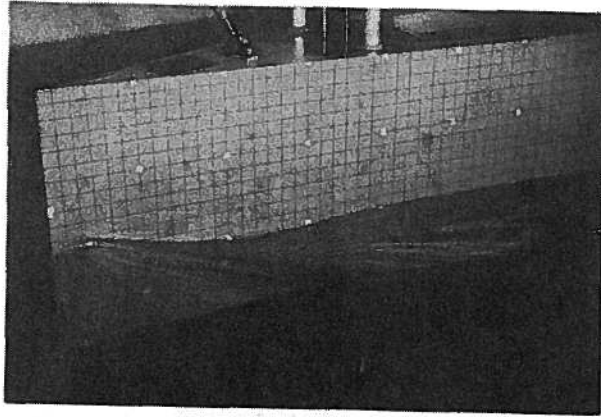


$U = 11.52$ ft./sec.

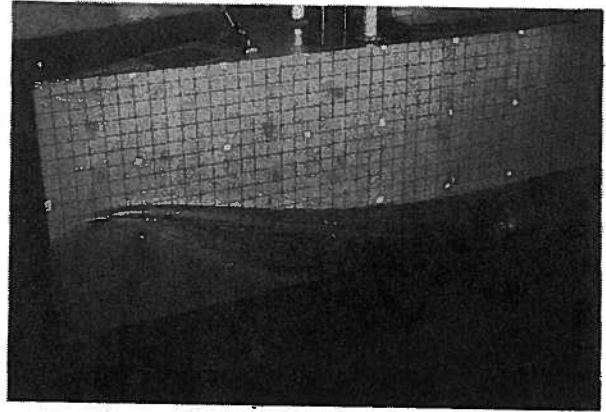


$U = 15.17$ ft./sec.

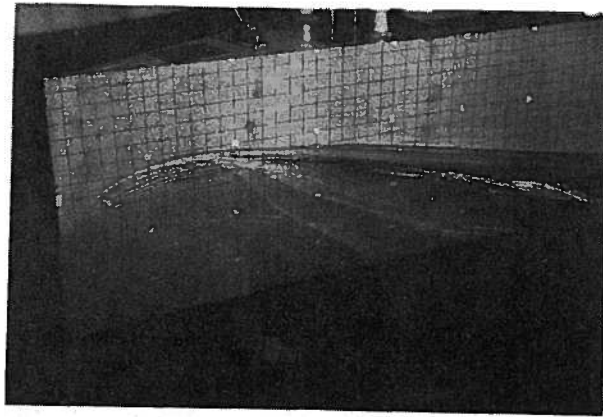
FIGURE 3. BOW WAVE ON A WEDGE
DRAFT = 12 IN. HALF ANGLE = 7.5°



$U = 3.64 \text{ ft./sec.}$



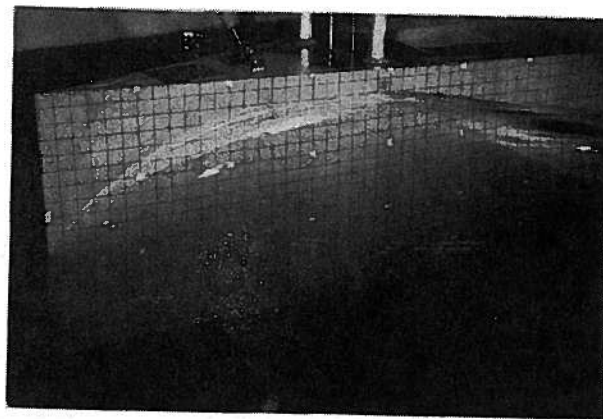
$U = 4.98 \text{ ft./sec.}$



$U = 7.64 \text{ ft./sec.}$



$U = 9.80 \text{ ft./sec.}$



$U = 11.46 \text{ ft./sec.}$

FIGURE 4. BOW WAVE ON A WEDGE

DRAFT = 12 IN.

HALF ANGLE = 15°

(iii) The corresponding rise in water level at the bow is greater for the wider-angle bow, but even in this case the level seems to stabilize at about 1.7 in. See Figure 4, parts (b) to (e), in which the rise varies between about 1.5 and 1.9 in. while the speed increases from 5.0 to 11.5 ft./sec. (Note: The white mark on the bow here is at the 16 in. draft.)

(iv) The region in which the bow wave dominates the picture increases steadily with forward speed. (The analysis predicts that the peak of the bow wave moves aft in proportion to U , the speed.) In the lowest-speed tests, there is a clear wave-trough behind the bow wave. See, for example, Figure 4, parts (a) and (b): The lowest visible white marks are on the still-water waterline. The trough is not predicted in the present analysis, and so we see that there are non-negligible waves at low speed which simply are not evident under the assumptions which have been made here. We cannot say whether the same kind of troughs occur at the higher speeds, because the model length was not great enough to observe the phenomenon.

From Figure 2, it was clear that we have a "universal" bow-wave curve which is supposed to apply to all wedges at all speeds at all drafts — within some unknown limits. To check this conclusion quantitatively, we measured just the amplitude and longitudinal position of the peak of the bow wave. For the finer wedge, the results for the wave amplitude are shown in dimensional form in Figure 5; the corresponding data for the longitudinal position of the peak are shown in Figure 6. These dimensional data are shown only to provide the reader with an impression of the scale of what was observed. The nondimensional wave-peak data are shown in Figure 7; according to the analysis, the nondimensional amplitude, Z_{\max} , should always have the same value, approximately 1.6. Figure 7 shows clearly that this is only roughly substantiated in the experiments. In fact, there are two ways in which the analysis is obviously deficient:

1) The assumption that made our analysis distinct from the usual slender-body theory was that the bow flow is essentially a "high-Froude-number" problem, in some sense. The depth-Froude-number is the only reasonable Froude number to consider in the bow region, and one can hardly expect the analysis to give good answers when $F_H \rightarrow 0$. In fact, it gives terrible answers then!

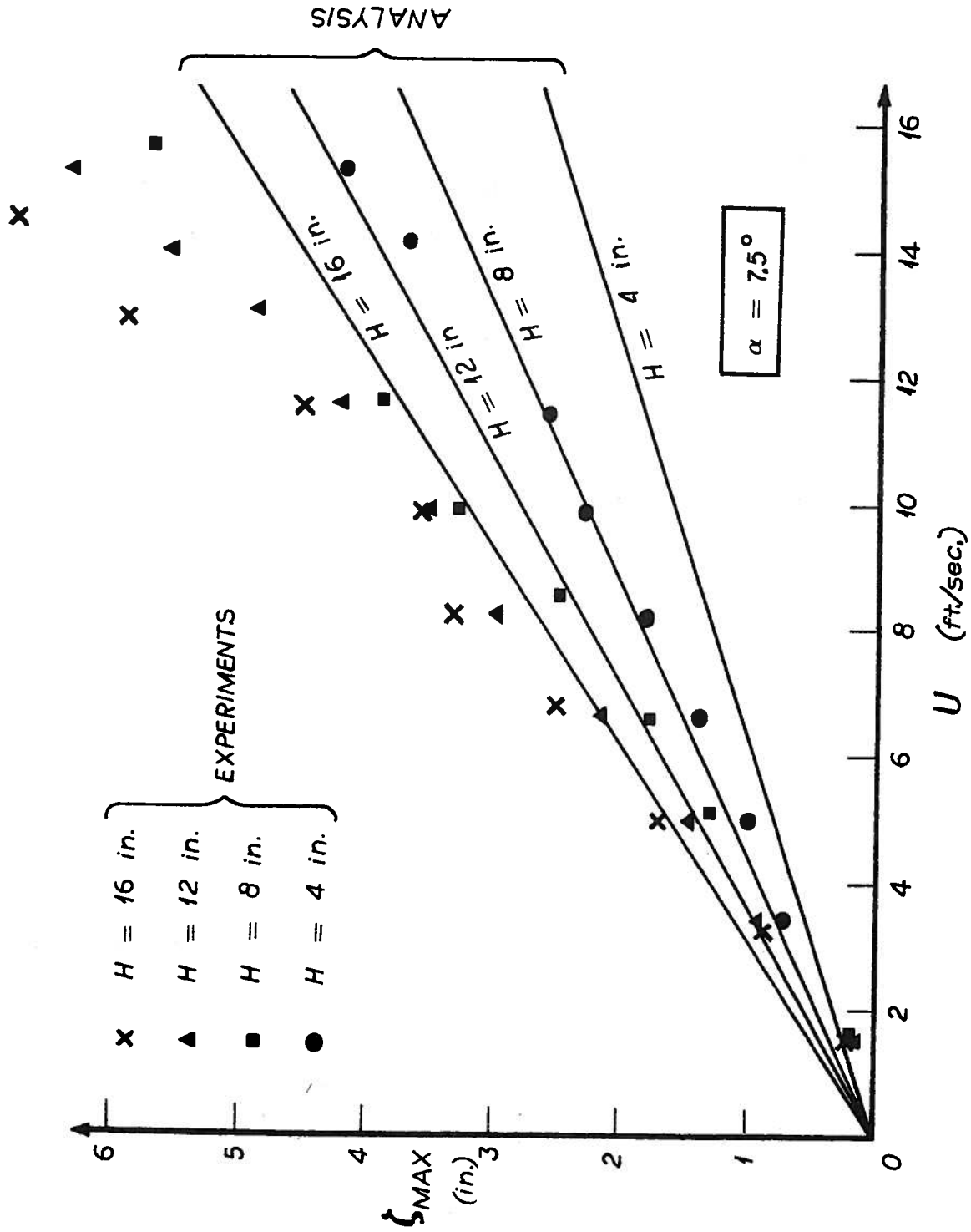


FIGURE 5. BOW WAVE AMPLITUDE ON WEDGE

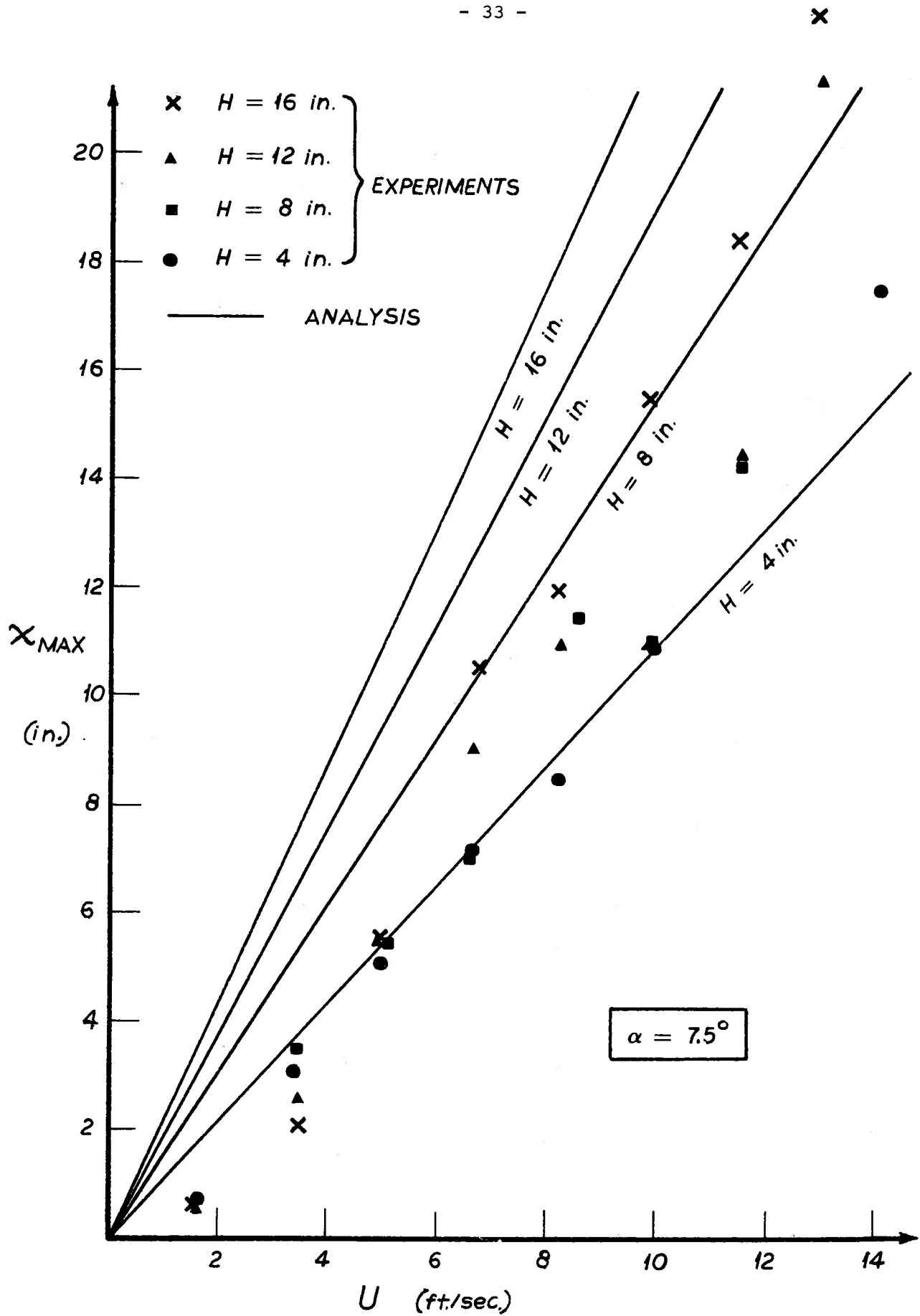


FIGURE 6. LONGITUDINAL POSITION OF WAVE PEAK

2) At the higher Froude numbers, the wave peak occurs at a considerable distance from the bow, at a place where the "thin-ship" representation of the body is probably quite invalid. We used the "thinness" twice, first in satisfying the body boundary condition approximately, then in evaluating the wave height on the body. (We simply set $y = 0$ in passing from (16) to (16').) The worse agreement for the wider wedge suggests that this "thinness" assumption may well be the cause of the increasing error at high Froude number.

If F_H is below some moderate value, it can be seen from Figure 7 that our method of nondimensionalizing the data seems to be still valid even when the Froude number drops below the level at which the analysis is valid. The reason for this is not clear, but the fact may be useful in reducing experimental data, even in cases in which the present analysis is obviously invalid.

The inaccuracy of the wave height predictions at high Froude numbers can probably be ameliorated if not completely removed by the introduction of a more precise method of solution of the problem. In principle, it appears to be possible to solve the bow-flow problem without introducing the thinness assumption, and some efforts have already been made to do just this. At the moment, however, we have no results to show for this effort.

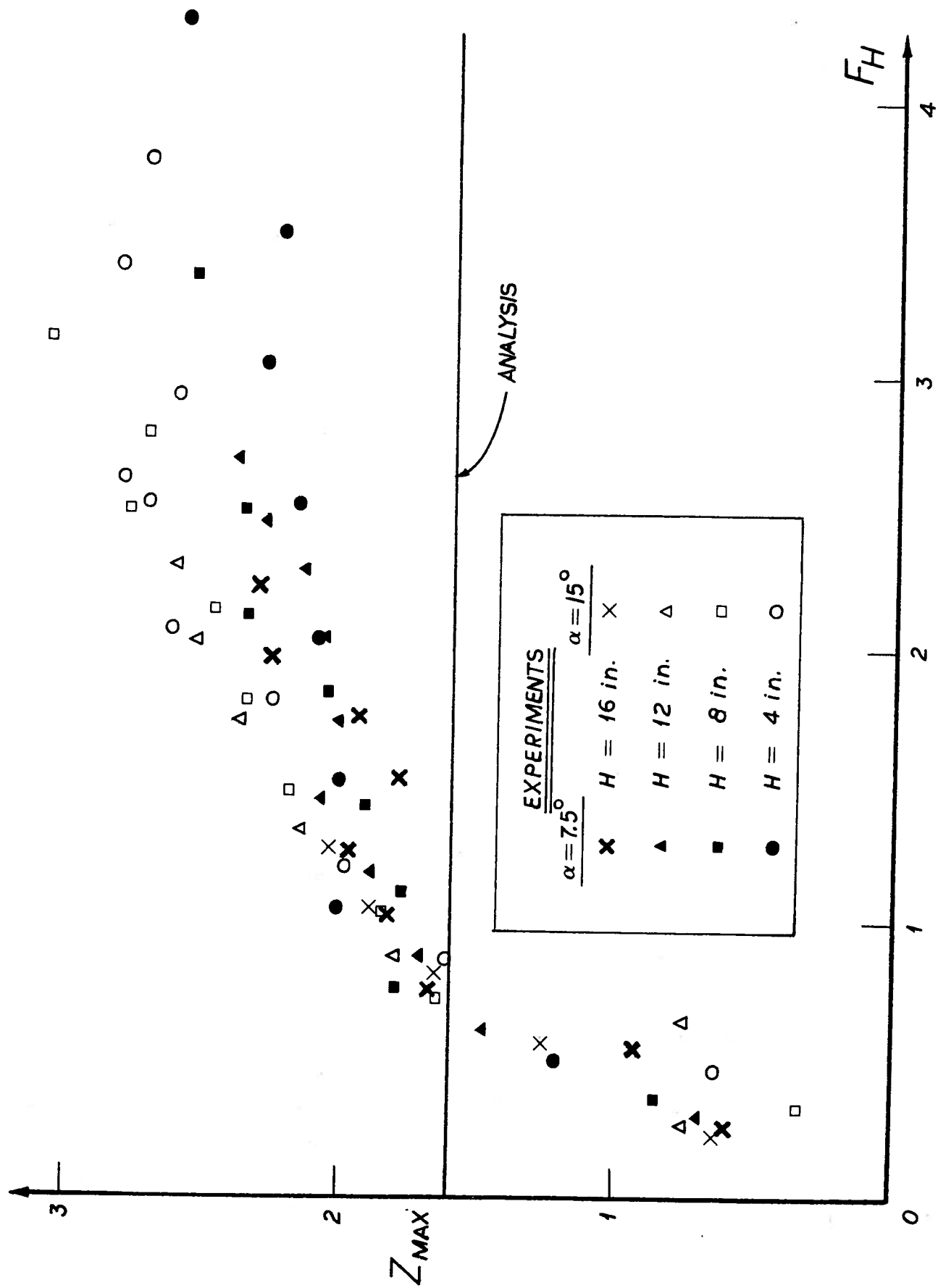


FIGURE 7. BOW WAVE AMPLITUDE (IN NONDIMENSIONAL FORM)

CRITIQUE OF THE ANALYSIS

Intuitively, we visualize a "slender body" as a body of which the length is much greater than the transverse dimensions. In addition, if we want to be a bit more precise, we require that there be no sudden changes in cross-section size or shape.

For such bodies, slender-body theory is likely to lead to reasonable predictions concerning a fluid flow around the body — provided we do not examine too closely what is happening near the ends of the body. The last qualification is necessary because slender-body theory is based on one major assumption which is usually violated near the body ends: It is assumed that the rates of change of all flow variables are much greater in the transverse directions than in the longitudinal direction. For a body with cusped ends, this assumption is valid even in the region near the ends, but the assumption is not valid near the body ends for most bodies of practical interest. The result is that slender-body theory typically predicts some kind of singular flow near the body ends.

Such a result is not necessarily unacceptable. If the singularities are integrable in some appropriate fashion and if the solution is approximately correct in most of the flow region, the presence of singularities in the mathematical solution may not even be serious. If one is very careful in obtaining the singularity strengths, one can even make some reasonable calculations concerning the flow around a blunt body in an infinite fluid. At cross-sections not too near the ends, the presence of singularities in the solution for the body end regions manifests itself as a perturbation of the longitudinal velocity component; this effect is rather minor over most of the body surface, and its precise evaluation is carried out by matching the near-field and far-field solutions.

In the free-surface problem, this procedure leads to an essential difficulty: In the far-field problem, the disturbance caused by the presence of the body appears actually to be caused by a line distribution of sources along the x axis, this axis lying in the plane of the undisturbed free surface. A concentrated source in the plane of the free surface is completely intolerable, because it causes much more than just local problems. (For example, the wave resistance of such a source is infinite.) Therefore we cannot hope to represent end effects in the simple way that is sometimes so successful for bodies in an

infinite fluid. In particular, we note the following important fact: No matter how nonlinear the local flow around the bow of the body may be, it cannot appear from afar as if it had been caused by a concentrated source.

In fact, an even stronger statement is possible: If, in the far field, the disturbance appears to have been caused by a line distribution of sources, the distribution must have a density which varies continuously. For the wedgelike body considered in this paper, slender-body theory predicts that the source density in the far-field expansion should have a jump at the bow. Actually, there may be a steep rise in the curve of source density, but there can be no jump in value. Otherwise the whole far-field solution has little meaning. *The far-field solution must be less singular at the bow than one might expect from infinite-fluid slender-body theory.*

There is another point of view which also encourages some optimism for treating the free-surface problem. The local behavior at the nose of a body in an infinite fluid appears to be intrinsically a three-dimensional problem. The presence of the body must have a fairly significant upstream influence. However, the additional presence of a free surface should reduce such upstream influences. Moreover, the isobaric property of the free surface may tend to smooth out variations in the longitudinal direction. Thus, one may be greatly encouraged to attempt to analyze the ship problem by slender-body theory.

These rationalizations have come, for the most part, after the preceding analysis had been developed and found to compare fairly well with experiments. Originally the motivation had been more like that described in the *Introduction*. In any case, we have found fair agreement between the analysis and our experiments, and so we should proceed to investigate further the internal consistency of the analysis, while we also investigate possible modifications and check them against experiments.

In the analysis as presented here, one may observe that the solution in the "bow near field" was never matched directly with the usual far-field solution of slender-ship theory. As Hirata [4] discovered, this is no small task. I have not yet carried out this matching, but I assume that it would lead only to a modification of the far-field source density in the neighborhood of the ship bow. Presumably, the source density curve would be rounded over in a region of length $O(\epsilon^{1/2})$ near the bow. Thus it would be possible to compute

the wave resistance of this shape of ship. (We have no assurance that the value computed would be accurate, but it would be a big improvement over ordinary slender-ship theory, which would give an infinite value of wave resistance for the ship with wedgelike bow!)

We have made only a few crude attempts to predict what happens just ahead of the edge of the wedge, and these attempts have not been described. Using a very heuristic mathematical model, I concluded at one time that the rise in water level ahead of the bow should be independent of forward speed (for a given wedge angle), and it was this tentative conclusion that led us to examine our photographs carefully, after which we came to a conclusion that there must be some truth in the crude analysis, since the water rise is in fact quite insensitive to forward speed.

The fact that the analysis is linear is, of course, a great help in obtaining a solution, but the most casual observation of the physical situation (as in Figures 3 and 4) suggests that linearization may be a great oversimplification. In defense of the linearization in this analysis, I offer just two comments:

(i) It always seems reasonable to try a linear analysis of any problem. One must in any case trust experimental evidence for the justification of an analysis. In the present problem, it is evident that the linear analysis is not grossly wrong.

(ii) In many mathematical analyses of fluid mechanics problems, apparently unacceptable singular solutions often become very useful when they are properly interpreted. I have already mentioned the appearance in slender-body theory of flow singularities which result from the invalidity of the assumptions in the regions near the body ends. Perhaps an even more interesting situation arises in some problems in which we find that the solution to a linearized problem represents approximately the correct flow patterns — but in slightly wrong places. Our bow-flow solution, for example, is not so singular as that which results from the usual slender-body theory, but it is still singular. It is interesting to note that the experimental data in Figure 6 would have a more orderly appearance if the ordinate scale had started at about $x_{\max} \approx -2$. In other words, the predictions in Figure 6 are considerably improved if we

arbitrarily assume that the rise in water level should have been measured from a point about 2 in. ahead of the bow. To this extent, our linearized results follow the pattern mentioned above: They are approximately correct, but in the wrong place.*

The form chosen for the solution in (1) is not an essential part of the analysis presented in this paper. It was an easy way to arrive quickly at a solution for a particular case. It has already been mentioned that this simplification may be at least partly responsible for the discrepancy between analysis and experiments at the higher Froude numbers. Having now determined that we have found some general agreement between analysis and experiments, we shall next try to obtain more precise solutions for these and similar problems. For example, the body cross-section shown in Figure 1 (either (a) or (b)) can be mapped into an auxiliary plane in which body and free surface together make up the horizontal axis. The free-surface condition must be transformed, of course, and then an integro-differential equation comparable to (3) can be obtained. This procedure can also be followed for bodies which are not symmetrical or for bodies which have an angle of attack. No solutions have been obtained yet except for that described by Hirata [4] for the case of a plate of zero thickness with an angle of attack. I hope that we shall be able to obtain solutions for several more realistic situations — for which comparisons with experimental data will provide more definitive evaluations of the fundamental approach described in the present paper.

*A more careful study of Figure 6 shows that the predicted curves have the correct slopes if the origin is placed on a sliding scale, with essentially no shift for the case of small draft, up to a shift of about 5 in. for the maximum draft case. I do not want to try to read too much quantitative significance into this result, however.

REFERENCES

- [1] T. F. Ogilvie, "Nonlinear High-Froude-Number Free-Surface Problems, *Jour. Engin. Math.*, **1** (1967) 2.5-235.
- [2] G. Vossers, *Some Applications of the Slender Body Theory in Ship Hydrodynamics*. Ph. D. thesis, 1962, Technical University of Delft.
- [3] W. P. A. Joosen, "Slender Body Theory for an Oscillating Ship at Forward Speed, : *Fifth Symposium on Naval Hydrodynamics, ACR-112*, 1964, pp. 167-183, Office of Naval Research, Washington, D. C.
- [4] M. H. Hirata, *On the Steady Turn of a Ship*. Ph.D. thesis, 1972, The University of Michigan.
- [5] E. Baba, unpublished manuscript, 1971.
- [6] H. Maruo, "High- and Low-Aspect Ratio Approximation of Planing Surfaces," *Schiffstechnik*, **14** (1967) 57-64.
- [7] M. J. Lighthill, *Fourier Analysis and Generalised Functions*, 1959, Cambridge University Press, Cambridge.
- [8] E. O. Tuck, "A Systematic Asymptotic Expansion Procedure for Slender Ships," *Jour. Ship Research*, **8:1** (1964) 15-23.
- [9] M. Abramowitz and I. A. Stegun, Ed., *Handbook of Mathematical Functions*, Applied Mathematics Series - 55, National Bureau of Standards, 1964, Washington, D. C.

DOCUMENT CONTROL DATA - R & D

(Security classification of title, body of abstract and indexing annotation must be entered when the overall report is classified)

1. ORIGINATING ACTIVITY (Corporate author) UNIVERSITY OF MICHIGAN, Dept. of Naval Architecture and Marine Engineering, Ann Arbor, Michigan 48104	2a. REPORT SECURITY CLASSIFICATION UNCLASSIFIED
	2b. GROUP

3. REPORT TITLE

THE WAVE GENERATED BY A FINE SHIP BOW

4. DESCRIPTIVE NOTES (Type of report and inclusive dates)

Interim Technical Report

5. AUTHOR(S) (First name, middle initial, last name)

T. Francis Ogilvie

6. REPORT DATE October 1972	7a. TOTAL NO. OF PAGES 45	7b. NO. OF REFS 9
------------------------------------	----------------------------------	--------------------------

8a. CONTRACT OR GRANT NO. N00014-67-A-0181-0033 b. PROJECT NO. SR 009 01 01 c. d.	9a. ORIGINATOR'S REPORT NUMBER(S) No. 127
	9b. OTHER REPORT NO(S) (Any other numbers that may be assigned this report) none

10. DISTRIBUTION STATEMENT

Approved for public release; distribution unlimited.

11. SUPPLEMENTARY NOTES	12. SPONSORING MILITARY ACTIVITY Naval Ship Research and Development Center, Washington, D. C. 20034
-------------------------	--

13. ABSTRACT

The flow field near the bow of a ship has some characteristics of a high-Froude-number problem, even if ship speed is moderate. Some of these features can be predicted by slender-body theory if the usual assumptions of that theory are modified in the bow region to allow for the occurrence of longitudinal rates of change greater than normally assumed. Analytical results are derived for the case of a fine wedge-shaped bow, in which case a universal curve can be drawn for the shape of the bow wave on the hull, regardless of speed, draft, or entrance angle (all within limits, of course). The lengths must be nondimensionalized by the quantity $(HU^2/g)^{1/2}$, where H is the draft, U is ship speed, and g is the gravitation constant. It is shown how this mathematical model matches with the usual slender-body model and how it eliminates certain of the objectionable features of the latter, with only minor complications. Some experimental results are shown which generally confirm the predictions.

14. KEY WORDS	LINK A		LINK B		LINK C	
	ROLE	WT	ROLE	WT	ROLE	WT
Ship Waves Bow Waves Maneuvering						

The University of Michigan, as an equal opportunity/affirmative action employer, complies with all applicable federal and state laws regarding nondiscrimination and affirmative action, including Title IX of the Education Amendments of 1972 and Section 504 of the Rehabilitation Act of 1973. The University of Michigan is committed to a policy of nondiscrimination and equal opportunity for all persons regardless of race, sex, color, religion, creed, national origin or ancestry, age, marital status, sexual orientation, gender identity, gender expression, disability, or Vietnam-era veteran status in employment, educational programs and activities, and admissions. Inquiries or complaints may be addressed to the Senior Director for Institutional Equity and Title IX/Section 504 Coordinator, Office of Institutional Equity, 2072 Administrative Services Building, Ann Arbor, Michigan 48109-1432, 734-763-0235, TTY 734-647-1388. For other University of Michigan information call 734-764-1817.